IOSR Journal of Engineering (IOSRJEN) **www.iosrjen.org**
ISSN (e): 2250-3021, ISSN (p): 2278-8719
Vol. 13, Issue 7, July 2023, ||Series -I|| PP 01-12

Synthesis of Copper-Nickel Oxide for Supercapacitor Applications

Arhaan Desai
Hrishita Shah

Enrolled at
Dhirubhai Ambani International School

Prof. Dr. Anamika Vitthal Kadam
The Institute of Science, Dr. Homi Bhabha State University, 15, Madam Cama Road, Fort, Mumbai, Maharashtra.
Received 14 July 2023; Accepted 30 July 2023

Project Abstract
In the project, we describe and evaluates the process for synthesis of copper-nickel oxide nanoparticles through two different methods: hydrothermal and electrochemical deposition. Subsequently, it delves into methods of characterization for nanoparticles. Performing an electrochemical analysis on the synthesized nanomaterial, it evaluates its use as a supercapacitor.
Keywords: Nanoparticles, Hydrothermal, Electrodeposition, Synthesis, Copper-Nickel Oxide, Characterisation, Electrochemical, Capacitance, XRD

Acknowledgment
We often realize that the words become insufficient tools to express our feelings of gratitude and gratefulness to those people who become involved in shaping our future. However, it is indeed a matter of great pleasure to have an opportunity to give vent my feelings of gratitude to the people who contributed in some way to the work described in this project.
We would like to extend our heartfelt gratitude to **Prof. Dr. Anamika Vitthal Kadam** for guiding us on this project, and to the Physics department of the Institute of Science, Mumbai for the use of their physical vapour deposition laboratory. Furthermore, we would like to thank our school, Dhirubhai Ambani International School, Mr. Amar Jadhav, Mr. Sharad Jadhav and the other PhD students studying at the Dr. Homi Bhabha State University for their guidance through this process.
Arhaan Desai and Hrishita Shah

I. Synthesis of the Nanoparticle

1.1 Introduction

1.1.1 Nickel Oxide

Nickel oxide (NiO) is a versatile transition metal oxide with various applications, with a large bandgap, and interesting electrochemical properties. It has a variety of structures, including nanoparticles, nanorods, nanosheets etc. As a p-type semiconductor, NiO generally has a bandgap of 3.6 to 4.0 eV. This wide bandgap allows it to be suitable for photocatalysis and optoelectronic devices. Its ability to undergo reversible redox reactions involving the conversion between Ni (II) and Ni(III) oxidation states, characterised by a colour change from transparent to dark brown. This enables NiO to function as an ideal substance for use in Li-ion batteries, supercapacitors, and electrochromic devices. At low temperatures, it is noted that NiO presents a better performance, one that is denoted by UV-vis spectroscopy and CV measurement.

1.1.2 Copper Oxide

Cuprous oxide, commonly referred to as copper (I) oxide, is an inorganic compound. Its chemical formula is as follows: Cu_2O. It is a reddish solid, with a very high melting point of approximately 1,235 °C. It acts as a p-type semiconductor, and has a narrow band gap of approximately 6.31 g/cm^3. It has several applications, for example as a semiconductor in photovoltaic devices, especially solar cells, as well as during the synthesis of diverse organic compounds, such as alcohols and carboxylic acids, where it acts as a catalyst.

1.2 Substrate Cleaning Process

Prior to the synthesis, cleaning the instruments and identifying the correct steel type to be utilised is vital. For all reactions carried out in the experiment, Stainless Steel (Type 304) was used due to its high corrosion resistance. After it was cut as per required (1 cm by 4 cm), the steel was cleaned. The surface of the substrate was smoothed and polished through the use of Flint Paper. Following this, it was cleaned with tap and double distilled water, and was submerged in dilute HCl (HCl: Water = 10:30 cm^3). Once again, the steel substrate was cleaned with double distilled water, and cleaned in acetone. After this, distilled water was added to a beaker, containing the cleaned substrates. This beaker was then placed in the ultrasonic machine for 20 minutes to further rid any impurities.

1.3.1 Experimental Setup

After all the apparatus - beakers, funnel, magnetic stirrer - is washed and cleaned as outlined before, the process of creating the precursor solution can start. The precursor solution was a mixture of cupric nitrate trihydrate solution ($Cu(NO_3)_2 \cdot 3H_2O$) and nickel nitrate trihydrate solution ($Ni(NO_3)_2 \cdot 6H_2O$). First, calculations were performed to obtain the ideal molar weight of each compound in the solution, using the formula:

$$\textbf{\textit{Molar weight}} = \frac{Molarmass \times Molarity \times volume}{1000}$$

25 ml of distilled water was added to 1.812gm of cupric nitrate, to form a 0.3M solution, and placed in a beaker atop a magnetic stirrer and left for a duration of 10 minutes. 25 ml of distilled water was added to 2.907gm of nickel nitrate to form a 0.4M solution, and slowly added to the cupric nitrate solution while it was being stirred. 5 ml of distilled water was added to 0.120gm of urea to form a 0.4M solution, and slowly added to the mixture while still being stirred. Following this, the precursor solution was tested using a pH paper indicator, and the pH was made to be constant at 7 through the addition of ammonium hydroxide. All the above precursor solution were used for both of the following methods.

Fig. 1.1 - Filtration for preparation of precursor solution

1.3.2 Hydrothermal Method

The hydrothermal method is a popular technique for synthesising nanoparticles using aqueous solutions at elevated temperatures and pressures.[1] It involves the controlled growth of nanoparticles through the dissolution and reaction of precursor materials in the solution. An insoluble material at ambient temperature is made soluble through this method, because of a high pressure environment curated due to higher temperature. This change and

[1] https://linkinghub.elsevier.com/retrieve/pii/S0963996918305945

growth takes place in an apparatus called an autoclave. This is a pressurised vessel, where the precursor solution forms deposits on the steel substrate.

The precursor solution made in section 1.3.1 was filtered. The stainless-steel substrates were removed from the ultrasonic cleaner and rinsed with double distilled water once again. They were then placed inside the teflon-lined autoclave vessel. Following this, the pale green filtrate of the precursor solution was added to the steel substrate in the autoclave. The autoclave was then bolted shut tightly, and placed in the muffle furnace at 110ºC for 4 hours. Once completed, the steel substrates were removed and dried at room temperature for 15 minutes. This was then annealed at 300ºC for 2 hours to provide a thin nanomaterial deposit.

Fig. 1.2 - Autoclave inside muffle furnace

1.3.3 Electrodeposition Method

The electrodeposition method, also referred to as electrochemical deposition, is another well-known technique for the synthesis of nanoparticles. This method enables us to obtain desired nanoparticles with a high purity, and also allows us to easily control the particle size by adjusting the current density.[2] For this method, the precursor solution made in section 1.3.1 was first filtered. It was then placed in a 10ml beaker. Next, two stainless steel substrates, as cleaned in section 1.2 were placed in the solution. A circuit was created with a power supply, connected voltmeter and ammeter, and positive and negative terminals. Following this, a substrate was made to act as the anode as it was connected to the positive terminal, serving as a reference, and the other substrate connected to the negative terminal formed the cathode where the deposition would take place. As the circuit was turned on with a voltage of 3.7V, deposition started to occur on the cathode. The positively charged ions at the anode are attracted to the cathode where they become neutral and form a layer or coat as they are deposited to form a pale blue-green layer. The steel substrate with the nanoparticle deposited on it was then rinsed with distilled water and dried at room temperature for 15 minutes. This was then annealed at 300ºC for 2 hours to provide a thin nanomaterial deposit.

[2]https://www.researchgate.net/publication/6746624_Synthesis_and_Characterization_of_Stable_Organosols_of_Silver_Nanoparticles_by_Electrochemical_Dissolution_of_Silver_in_DMSO

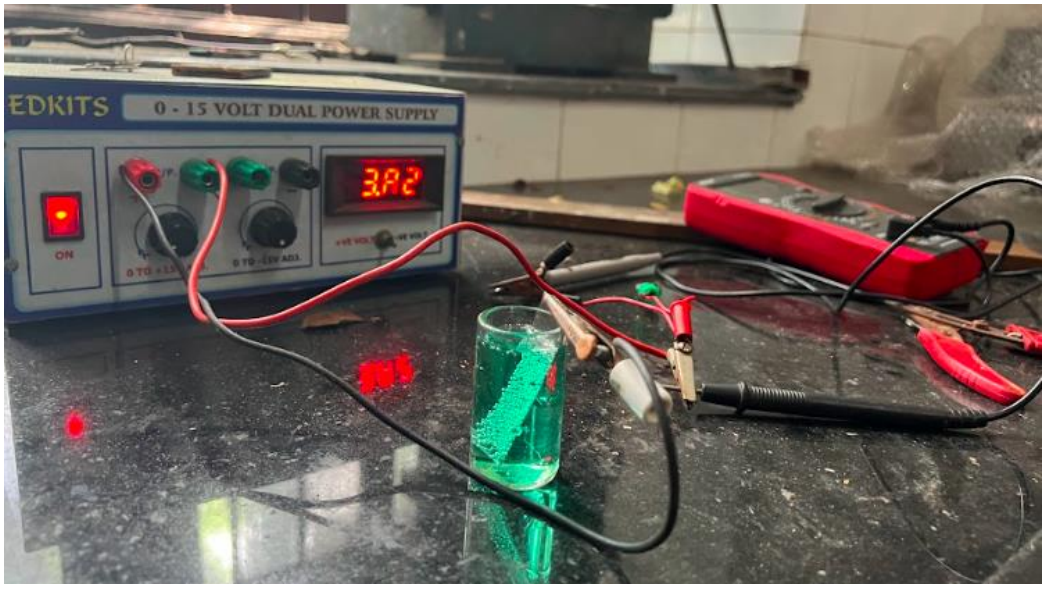

Fig. 1.3 - Circuit for electrodeposition method

1.3.4 Results and Evaluation

As displayed above, both methods resulted in the synthesis of the nanoparticle, but with a different thickness of deposit layers. Qualitatively, it can be concluded that the electrodeposition method yielded a better deposit owing to the thickness of the deposit layer and its dark black colour. For the subsequent characterization and electrochemical analysis, the copper nickel oxide synthesised through the electrodeposition method was thus utilised.

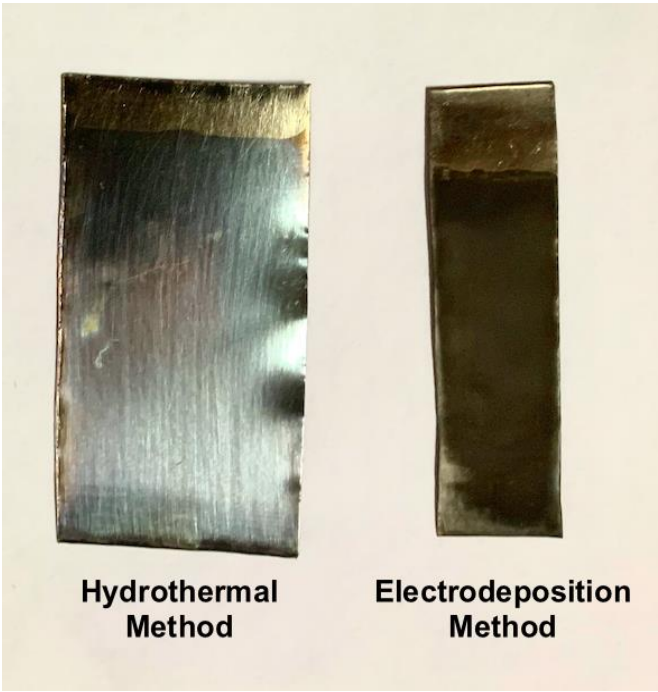

Fig 2 - Synthesised Nanomaterials by hydrothermal and electrodeposition method

II. Characterization of the synthesised nanoparticle

2.1 X-Ray Diffraction Analysis (XRD)

To visualise the chemical properties, physical composition, and crystallographic structure of the CuO NP synthesised, XRD is the ideal tool. It probes the structure on the atomic scale, with the machine consisting of 4 main components: Specimen stage, X-ray emitter, optics receiver, and X-ray detector.

Once the CuO NPs have been synthesised, the specimen is placed on the stage of the XRD machine. Electrons are accelerated towards a copper target as a high voltage is applied, resulting in the dislodgement of copper's inner shell electrons. As a result, outer-shell electrons drop their energy level and fill in any present vacancies, thereby releasing X-rays. These generated X-rays are directed towards the CuO NPs. To deduct the interplanar spacing and its effects, monochromatic radiation-based X-rays are used. Upon collision, the rays are diffracted and scattered at various angles. The X-ray detector detects the diffracted rays and measures their intensities at different angles. This produces a diffractogram, which is interpreted using Bragg's Law: $2d \sin\theta = n\lambda$ (Eq. 1),[3]where 'd' is the lattice spacing, 'n' is the order of diffraction, 'θ' is the diffraction angle and 'λ' is the wavelength of the monochromatic x-ray.[4] Using the characterised values of θ, n and λ, we can calculate the 'd' values. Following indexing of the XRD peaks, each is assigned their respective Miller indices and then compared with the Joint Committee on Powder Diffraction Standards (JCPDS) database.[5] The characterization is also taken further to determine the average crystallite size through the Sherrer formula: $\square = \frac{\square k}{\beta\square\square\square\square}$ (Eq. 2)[6], where D is the average particle size, λ is the wavelength of radiation (1.0542 Å (Cu Kα)), θ is Bragg's Angle and β is the Full Width at Half Maximum (FWHM) of the reflection peak, and k is the Sherrer constant. The values of K range from 0.89 to 1.39 but is generally considered as 0.9. Thus, the XRD analysis tool is extremely beneficial in enabling the determination of crystal structure, crystallite size and phase that allow the characterization of CuO NPs to occur.

Fig 3.1 - XRD Machine

2.2 Ultraviolet Visible Spectroscopy (UV-Vis Spectroscopy)

UV-Vis Spectroscopy is a technique based on the absorption of light in the UV-visible region of the electromagnetic spectrum by nanoparticles. This method characterises CuO NPs' electronic structure, concentration, band gap energy and size distribution. UV-Vis Spectroscopy relies on the fundamental interaction between electromagnetic radiation and matter. Beams of light passing through the CuO sample are absorbed as the photon energy matches the energy difference between the ground and excited electronic states of the atoms within the NPs.[7] This absorption of light results in the excitation of CuO's electrons from the ground state to an excited one. The amount of light absorbed is quantified through the Beer-Lambert Law: $A = \varepsilon Lc$ (Eq. 3), where

[3] https://www.xtal.iqfr.csic.es/Cristalografia/archivos_10/Bragg-firstpaper-mini.pdf

[4] https://lufaso.domains.unf.edu/

[5] https://www.cambridge.org/core/journals/powder-diffraction/article/abs/jcpds-international-centre-for-diffraction-data-sample-preparation-methods-in-xray-powder-diffraction/E959F6D80796DB1D5DFFEA55C7C8E844

[6] https://www.scirp.org/journal/paperinformation.aspx?paperid=23195

[7] https://amslaurea.unibo.it/18799/1/Study%20of%20the%20Growth%20of%20Ultrathin%20LiF%20Films%20on%20Ag(100)%20-%20Romankov%20Vladyslav.pdf

A is the absorbance, ε is the molar absorptivity, L is the path length and c is the concentration of the compound in solution.[8] To perform UV-Vis Spectroscopy, a UV-visible spectrophotometer is utilised, measuring the intensity of light transmitted through a sample compared to a reference measurement of the incident light source.[9] The spectrophotometer consists of four main components: a light source, a monochromator, a beam splitter, and a detector.

Following calibration of the spectrophotometer using a reference or blank material, a small volume of CuO is transferred into a cuvette. Light from deuterium and tungsten lamps is incident on the monochromator, which is refracted into a rainbow of colours. Only one wavelength of light passes through the slit following interaction with the monochromator. The light is then incident on the beam splitter, which equally distributes the light to pass through both the cuvettes (the reference material as well as the CuO cuvette). The detector then measures the intensity of transmitted light providing a spectrum that delineates the absorbance of NPs at various wavelengths. The peak absorbance characterised is used to calculate the band gap energy of the CuO NPs using the formula: $E_g = 1240/\lambda$ (Eq. 4), where E_g is the band gap energy, and λ is the wavelength.

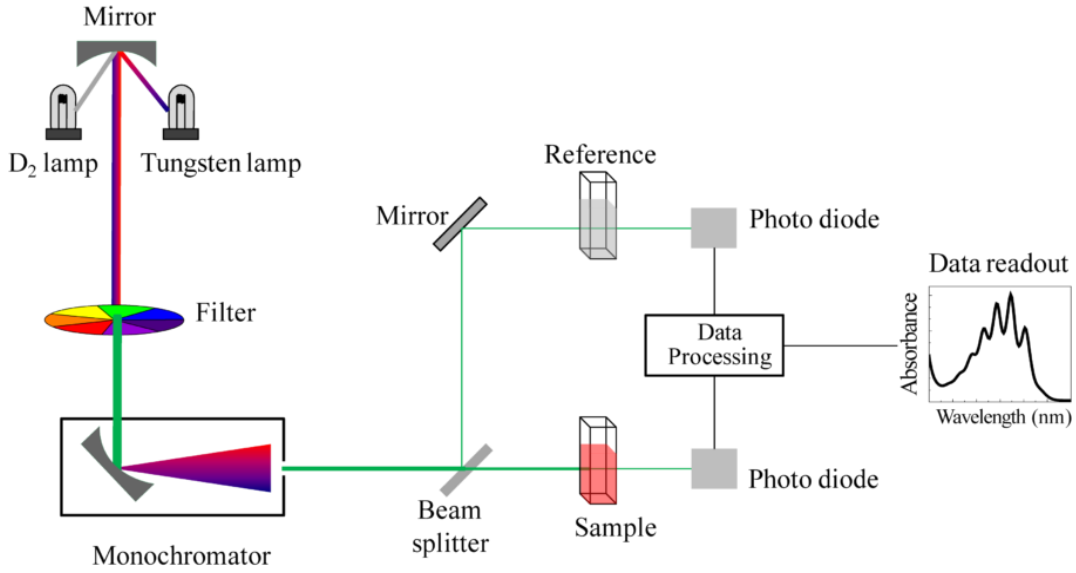

[10]

Fig 3.2 - UV-vis Spectroscopy

2.3 Fourier Transform Infrared Spectroscopy

Fourier Transform Infrared Spectroscopy, henceforth referred to as FTIR, is a characterization technique that allows us to understand the internal structure of the synthesised copper oxide nanoparticles, with specific emphasis on the functional groups present on the nanoparticle. By analysing the infrared spectra obtained and correlating the peaks with particular functional groups, we can gain insights into those present on the synthesised nanoparticle. The FTIR spectrometer relies on an infrared light source, such as the Nernst glower or the tungsten glower, resulting in the emission of primarily mid-IR region wavelengths.

This radiation beam then enters the interferometer, or, more specifically, the Michelson interferometer - the main component of an FTIR spectrometer. This consists of three primary components - a beam splitter, a moving mirror and a fixed mirror. The infrared beam undergoes collimation and subsequently enters the beam splitter. Here, two beams are obtained - one 'sample beam' that passes through the synthesised nanoparticle and that is transmitted to the movable mirror, and one 'reference beam' to the fixed mirror. After travelling the two different paths, they recombine at the beam splitter, creating an interference pattern, which contains information about differences in the intensity of the infrared light caused by the sample. This constantly changing interference

8 https://chem.libretexts.org/Bookshelves/Physical_and_Theoretical_Chemistry_Textbook_Maps/Supplemental_Modules_(Physical_and_Theoretical_Chemistry)/Spectroscopy/Electronic_Spectroscopy/Electronic_Spectroscopy_Basics/The_Beer-Lambert_Law

[9] https://www.agilent.com/en/support/molecular-spectroscopy/uv-vis-uv-vis-nir-spectroscopy/uv-vis-spectroscopy-spectrophotometer-basics

[10] https://www.researchgate.net/figure/Schematic-of-UV-visible-absorption-spectroscopy-37_fig3_349441962

pattern is recorded by a detector, which produces an interferogram which is mathematically transformed using Fourier transform techniques to an infrared spectrum. Finally, this spectrum can be analysed to understand the molecular structure and functional groups present.

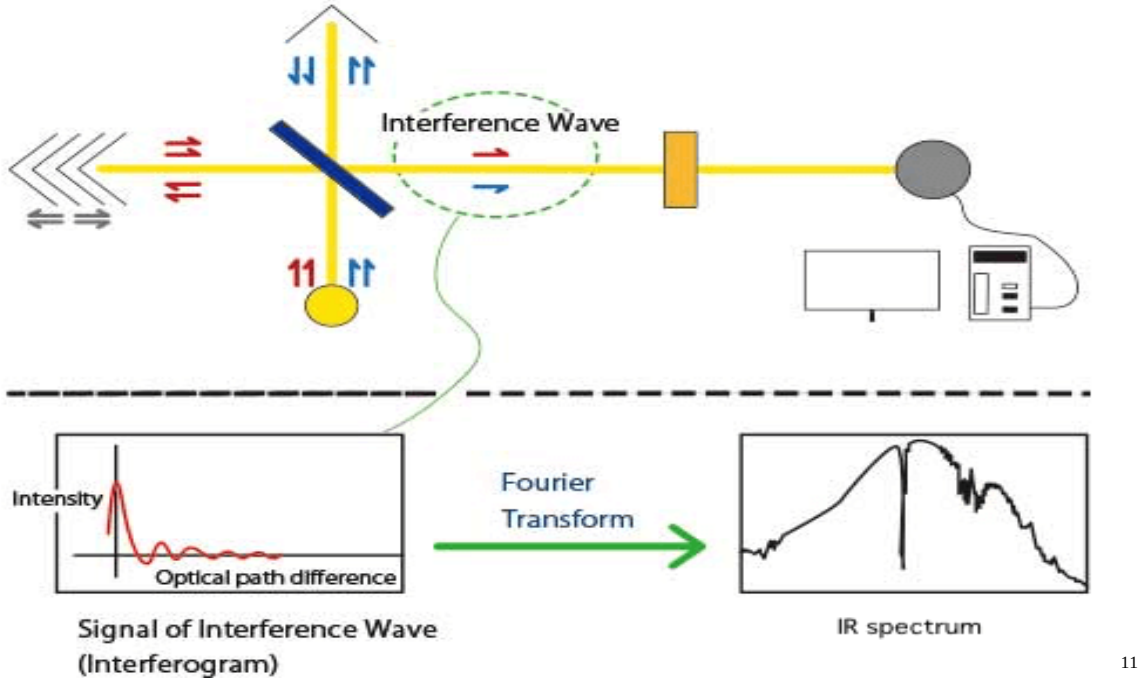

[11]

Fig 3.3 - Fourier Transform Infrared Spectroscopy

2.4 Scanning Electron Microscopy (SEM)

This characterisation process uses a beam of electrons to enable us to view microscopic details on the sample prepared. Differing from a light microscope in that the magnification is not limited by the wavelength of the light used for illumination, an electron microscope allows the viewer to observe a sample in much better detail - including the crystalline structure and surface morphology.

Functioning of the Scanning Electron Microscope:

The microscope starts with an electron source, usually a heated tungsten filament or a field emission electron gun, which emits a beam of high-energy electrons. Subsequently, these electrons pass through several electromagnetic lenses and coils which are responsible for controlling and focusing the beam by manipulating its trajectory to ensure it remains in a narrow vertical path and focused downwards towards the sample. The sample is placed within a vacuum chamber to prevent molecules or atoms already present in the microscope column from interacting with the electron beam.[12] When the electron beam hits the sample, X-rays and electrons are ejected, as seen in the image below:

[11] https://www.jasco-global.com/principle/principles-of-infrared-spectroscopy-4-advantages-of-ftir-spectroscopy/

[12] https://www.scimed.co.uk/education/sem-scanning-electron-microscopy/

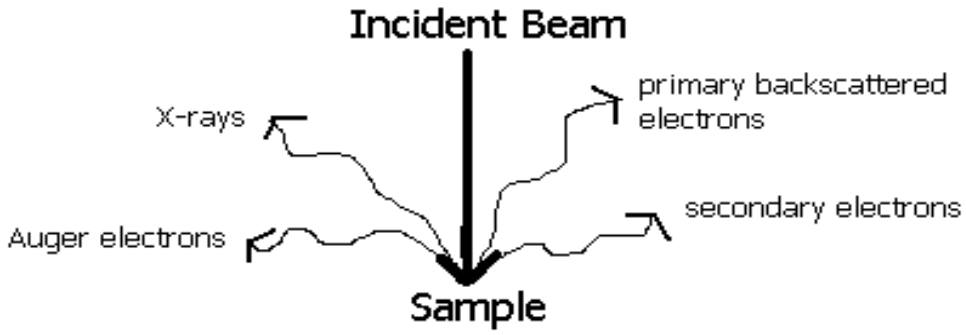

[13]

Fig 3.4 - Ejection of X-rays and electrons

These include backscattered electrons (high-energy electrons that are reflected back by the scattering of the primary beam electrons due to elastic collisions.[14]) and secondary electrons (electrons generated as ionisation products from inelastic collisions). These electrons along with the X-rays are detected by detectors in the microscope, from which the signals are then analysed, amplified and processed to form an image.

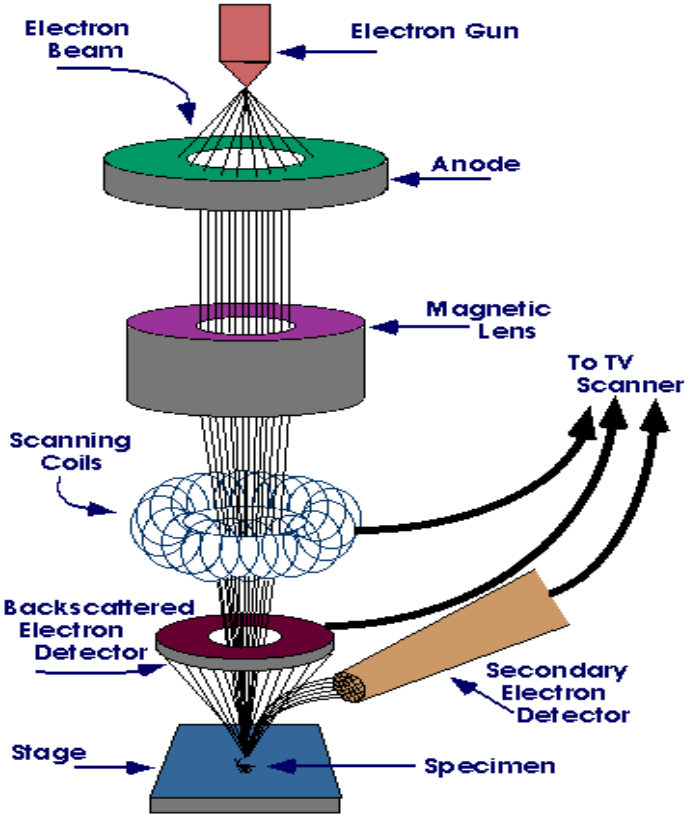

[15]

Fig 3.5 - Scanning Electron Microscope

[13] https://www.purdue.edu/ehps/rem/laboratory/equipment%20safety/Research%20Equipment/sem.html

[14] https://www.thermofisher.com/in/en/home/global/forms/industrial/backscattered-electrons-sem.html

[15] https://www.researchgate.net/figure/Fig-35-Schematic-diagram-of-the-scanning-electron-microscope-SEM_fig5_331989270

III. Electrochemical Analysis

Electrochemistry as a characterization and analysis technique deals with the collection of techniques that use electrical stimulation to analyse the chemical reactivity of a sample surface or a solution.[16] In this reaction, a cation of the reactive species is reduced or oxidised, thereby resulting in a generation of electrons and a current. This reaction occurs when the applied voltage is greater than the equilibrium voltage. This results in convention, wherein a positive current characterises an oxidation and a negative current characterises a reduction.

3.1 Process

A 3-electrode system was utilised to analyse the electrochemical characteristics. This setup featured a reference electrode and a working electrode as anodes, the synthesised substrate as the cathode, and the made aqueous Cu-Ni Oxide as the electrolyte. The system was connected to the electrochemical analyser, which was then connected to a computer that provided the data results. Through this system, in the absence of agitation, the movement of ions occurs due to migration and diffusion. Migration involves movement of ions due to an electric field, while diffusion involves the movement of ions due to a concentration gradient.[17] In the situation of Cu-Ni oxide NPs' electrochemical characterisation, migration causes the anions and cations to be displaced in directions opposite to each other, from one electrode to another. This results in insertion and/or absorption mechanisms, seen through cyclic voltammetry (CV). The produced CV curves allow us to calculate specific capacitance.

3.2 Specific Capacitance

Using the Chemical Analyser, 2 graphs are received based on varied scan rate (mV/s) and varied current density (mA/cm^2). The mass of nanomaterial used is constant (0.007g), as is the Potential (1.1V).

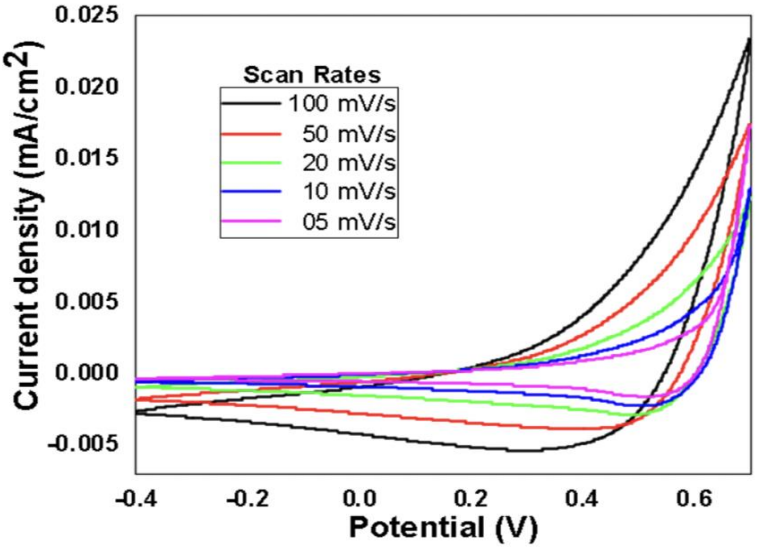

Graph 1 - Current Density vs Potential (Varied Scan Rate)

[16] https://www.eag.com/techniques/electrochemical-analysis/

[17] doi.org/10.1016/0022-0728(94)03404-4

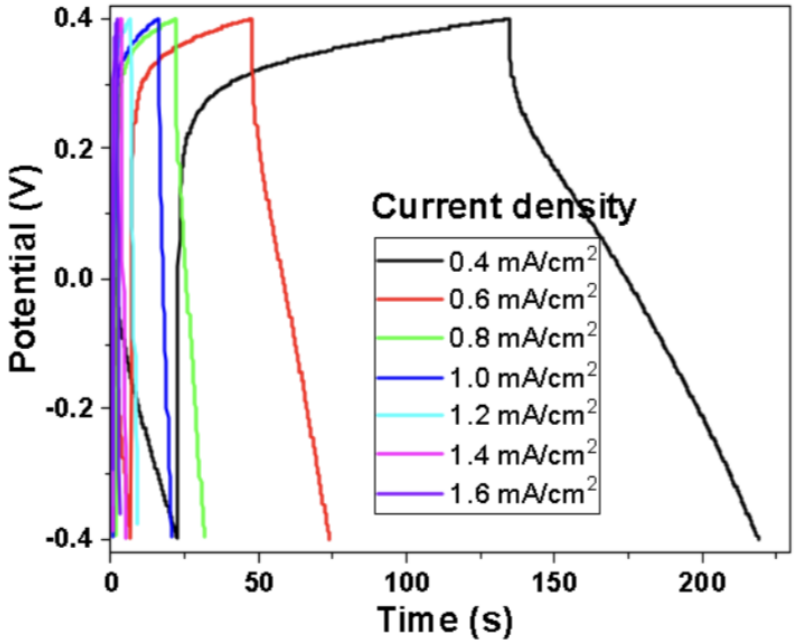

Graph 2 - Potential vs Time (Varied Current Density)

In order to calculate the specific capacitance, the following formula is used:

$$specific\ capacitance(C) = \frac{Area\ of\ CV\ Curves}{Mass \times Voltage \times S.R.}$$

Where: C is the specific capacitance, Q is the charge, m is the mass, v is the voltage, S.R. is the scan rate
Subsequently, to determine Q from the graph the following formula is used:

$$Q = \int_{V2}^{V1} f(t).dt$$

This results in the following data, displayed as a table below:

Table 1 - Relationship between scan rate and specific capacitance

Potential (V)	Scan Rate (mV/s)	Mass of nanoparticle (g)	Area (Q) (mA s)	Specific Capacitance (F / g)	Specific Capacitance (mF / g)
1.1	100	0.007	0.005523065185	0.007172812	7.172811929
1.1	50	0.007	0.004119121495	0.010699017	10.69901687
1.1	20	0.007	0.002855768700	0.018543953	18.5439526
1.1	10	0.007	0.001963280000	0.025497143	25.49714286
1.1	5	0.007	0.001219880300	0.031685203	31.6852026

IV. Conclusions

The nanomaterial synthesised was therefore capable of storing and releasing charge, with a maximum specific capacitance of approximately 31.69 mF/g when the scan rate was 5 mV/s. Thus, this nonmaterial can be used in a supercapacitor device, for example in smart phones and smart watches. Furthermore, from the above data table, we can infer that as the scan rate (in mV/s) increases, the specific capacitance decreases, delineating an inverse relationship.

References

[1]. Balamurugan, Jayaraman, Tran Duy Thanh, Seok-Bong Heo, Nam Hoon Kim, and JoongHee Lee. "Novel route to synthesis of N-doped graphene/Cu–Ni oxide composite for high electrochemical performance." Carbon 94 (2015): 962-970.

[2]. Bessi, A., B. Boudine, and C. Boudaren. "Fabrication and Characterization of TiO 2 Nanoparticles." In Proceedings of the Third International Symposium on Materials and Sustainable Development 3, pp. 296-300. Springer International Publishing, 2018.

[3]. Bréchignac, Catherine, Philippe Houdy, and Marcel Lahmani, eds. Nanomaterials and nanochemistry. Springer Science & Business Media, 2008.

[4]. Burgstaller, Wolfgang, Martina Hafner, Michael Voith, Andrei IonutMardare, and Achim Walter Hassel. "Copper–nickel oxide thin film library reactively co-sputtered from a metallic sectioned cathode." Journal of Materials Research 29, no. 1 (2014): 148-157.

[5]. Carnes, Corrie L., Jennifer Stipp, Kenneth J. Klabunde, and John Bonevich. "Synthesis, characterization, and adsorption studies of nanocrystalline copper oxide and nickel oxide." Langmuir 18, no. 4 (2002): 1352-1359.

[6]. Chauhan, Ashish, and Priyanka Chauhan. "Powder XRD technique and its applications in science and technology." J Anal Bioanal Tech 5, no. 5 (2014): 1-5.

[7]. Cioffi, Nicola, Nicoletta Ditaranto, Luisa Torsi, and LuigiaSabbatini. "Approaches to synthesis and characterization of spherical and anisotropic copper nanomaterials." Nanotechnologies for the Life Sciences: Online (2007).

[8]. Dupas, Claire, and Marcel Lahmani, eds. Nanoscience: Nanotechnologies and nanophysics. Springer Science & Business Media, 2007.

[9]. Edison, Thomas NesakumarJebakumar Immanuel, Raji Atchudan, and Yong Rok Lee. "Binder-free electro-synthesis of highly ordered nickel oxide nanoparticles and its electrochemical performance." Electrochimica Acta 283 (2018): 1609-1617.

[10]. Gan, Yong X., Ahalapitiya H. Jayatissa, Zhen Yu, Xi Chen, and Mingheng Li. "Hydrothermal synthesis of nanomaterials." Journal of Nanomaterials 2020 (2020): 1-3.

[11]. Goyal, Rajendra Kumar. Nanomaterials and nanocomposites: synthesis, properties, characterization techniques, and applications. CRC Press, 2017.

[12]. Khan, Hayat, Aditya S. Yerramilli, Adrien D'Oliveira, Terry L. Alford, Daria C. Boffito, and Gregory S. Patience. "Experimental methods in chemical engineering: X-ray diffraction spectroscopy—XRD." The Canadian journal of chemical engineering 98, no. 6 (2020): 1255-1266.

[13]. Li, Gao-Ren, Han Xu, Xue-Feng Lu, Jin-Xian Feng, Ye-Xiang Tong, and Cheng-Yong Su. "Electrochemical synthesis of nanostructured materials for electrochemical energy conversion and storage." Nanoscale 5, no. 10 (2013): 4056-4069.

[14]. Li, Ruizhi, et al. "Integrated copper–nickel oxide mesoporous nanowire arrays for high energy density aqueous asymmetric supercapacitors." Nanoscale Horizons 1.2 (2016): 150-155.

[15]. Morey, George W. "Hydrothermal synthesis." Journal of the American Ceramic Society 36, no. 9 (1953): 279-285.

[16]. Raliya, Ramesh, Vinod Saharan, Kailash Choudhary, Sudha Summarwar, Khushboo Gulecha, Vikal Gupta, and Prakash Mal Sain. "Nanomaterials synthesis and characterization." In Nanoscale Engineering in Agricultural Management, pp. 1-10. CRC Press, 2019.

[17]. Rassaei, Liza, Frank Marken, Mika Sillanpää, Mandana Amiri, Ciprian Mihai Cirtiu, and Markus Sillanpää. "Nanoparticles in electrochemical sensors for environmental monitoring." TrAC Trends in Analytical Chemistry 30, no. 11 (2011): 1704-1715.

[18]. Rocha, Fellipy S., Anderson J. Gomes, Claure N. Lunardi, Serge Kaliaguine, and Gregory S. Patience. "Experimental methods in chemical engineering: Ultraviolet visible spectroscopy—UV-Vis." The Canadian Journal of Chemical Engineering 96, no. 12 (2018): 2512-2517.

[19]. Rodriguez-Sanchez, L., M. Carmen Blanco, and M. Arturo López-Quintela. "Electrochemical synthesis of silver nanoparticles." The Journal of Physical Chemistry B 104, no. 41 (2000): 9683-9688.

[20]. Sharma, Kriti, Anmol Arora, and Surya Kant Tripathi. "Review of supercapacitors: Materials and devices." Journal of Energy Storage 21 (2019): 801-825.

[21]. Srivastava, Richa. "Synthesis and characterization techniques of nanomaterials." International Journal of Green Nanotechnology 4, no. 1 (2012): 17-27.

[22]. Therese, G. Helen Annal, and P. Vishnu Kamath. "Electrochemical synthesis of metal oxides and hydroxides." Chemistry of materials 12, no. 5 (2000): 1195-1204.

[23]. Vollath, Dieter. "Nanomaterials an introduction to synthesis, properties and application." Environmental Engineering and Management Journal 7, no. 6 (2008): 865-870.
[24]. Yin, J. L., and Jae Yeong Park. "Electrochemical investigation of copper/nickel oxide composites for supercapacitor applications." International journal of hydrogen energy 39, no. 29 (2014): 16562-16568.
[25]. Yin, J. L., and Jae Yeong Park. "Electrochemical investigation of copper/nickel oxide composites for supercapacitor applications." International journal of hydrogen energy 39, no. 29 (2014): 16562-16568.
[26]. Zaky, Ayman M., and Fawzi H. Assaf. "Cyclic voltammetric behaviour of copper–nickel alloys in alkaline media." British Corrosion Journal 37, no. 1 (2002): 48-55.
[27]. Zhang, Dongmei, Yuanming Zheng, Guangchen Yuan, Guoping Qian, Henglong Zhang, Zhanping You, and Ping Li. "Chemical characteristics analyze of SBS-modified bitumen containing composite nanomaterials after aging by FTIR and GPC." Construction and Building Materials 324 (2022): 126522.
[28]. Zhao, Xin, Beatriz Mendoza Sánchez, Peter J. Dobson, and Patrick S. Grant. "The role of nanomaterials in redox-based supercapacitors for next generation energy storage devices." Nanoscale 3, no. 3 (2011): 839-855.